JOURNAL OF MATERIALS SCIENCE 29 (1994) 2107–2114

Pull-out of short rods and fibres

A. N. GENT*
C. N. R. S. Centre de Recherches sur la Physico-Chimie des Surfaces Solides, 24 Avenue du President Kennedy, F-68200 Mulhouse, France

C. L. SHAMBARGER
The Goodyear Tire and Rubber Company, Lincoln Manufacturing Division P.O. Box 83248, Lincoln, NE 68501, USA

An experimental study has been carried out of the mechanics of pull-out of short nylon rods embedded in a rubber block, considered as a model of fibres embedded in an elastic resin. Two stages of pull-out were observed. First, rubber became detached from the base of the rod creating a large internal cavity. This process was apparently initiated by internal rupture of rubber under the rod, and occurred when the local triaxial tension reached a value similar to the tensile (Young's) modulus of the rubber. After cavitation, a cylindrical debond propagated up the rod, starting at the embedded end and ending in complete pull-out. Pull-out forces were found to be consistent with a simple fracture mechanics treatment based on the elastic compliance of partially debonded specimens, both measured and calculated by finite element analysis. The fracture energy for debonding is deduced to be about 300 $J\,m^{-2}$. The effects of varying rod diameter and depth of embedment are shown to be in satisfactory agreement with theory.

1. Introduction

Previous work has dealt with pull-out of a relatively long rigid rod or fibre lying along the axis of an elastic cylinder, Fig. 1 [1–5]. As a debond propagates up the fibre, starting at the embedded end, the part of the cylinder that becomes detached is assumed to become strained by the pull-out force, F. If it becomes strained uniformly, in simple extension say, then F is predicted to be constant, independent of the depth, l, of embedment and the extent of debonding, and given by

$$F^2 = 4\pi^2(R^2 - a^2)aEG_a \qquad (1)$$

where R is the radius of the elastic cylinder, a is the radius of the rod or fibre, E is the tensile (Young's) modulus of the material, and G_a is a characteristic energy required to debond a unit area of bonded surface. Good agreement is obtained with this simple result provided that the rod radius, a, is small and the depth, l, of embedment is large compared to the radius, R, of the elastic cylinder [1]. However, for rods with larger radii, friction at the already debonded interface can lead to an increasing pull-out force, sometimes much larger than that given by Equation 1 [2–4].

We now turn to another pull-out experiment, when the depth, l, of embedment is small compared to the radius, R, of the elastic cylinder in which the rod is embedded, Fig. 2. In this case it might be thought that the elastic material can be regarded as a semi-infinite half-space whose actual dimensions, radius, R, and thickness, H, are immaterial. In fact, however, as indicated by the numerical analysis described in the Appendix and corroborated by experiment, the size of the elastic block in which the fibre is embedded remains as a significant quantity affecting the pull-out force, even when the block dimensions are much larger than the rod radius, a, or depth, l, of embedment.

In all cases, pull-out of rods was preceded by cavitation in rubber underneath the flat end. These cavities then spread to cause total debonding of the flat end surface of the rod, and the applied force dropped simultaneously to a lower value. As the rod was pulled further, the force rose again somewhat, until the rod was pulled completely free.

Four basic measurements were made in the experiments.

(a) The slope of the initial linear relation between applied force, F, and displacement, d, of the rod before any cavity was seen and before any debonding occurred; this information was used to characterize the elastic behaviour of a block containing a fully-bonded rod.

(b) The force, F_c, at which cavitation occurred, taken as the maximum force reached before the onset of sudden cavitation; these results are compared with expected values for cavitation in rubber itself.

(c) The slope of the linear relation between applied force, F, and displacement, d, of the rod after cavitation was complete and the flat end was fully debonded; these results are employed to deduce the pull-out force by assuming that changes in compliance with embedded depth are equivalent to changes that occur

* *Permanent address*: Institute of Polymer Engineering, The University of Akron, Akron, OH 44325, USA.

0022–2461

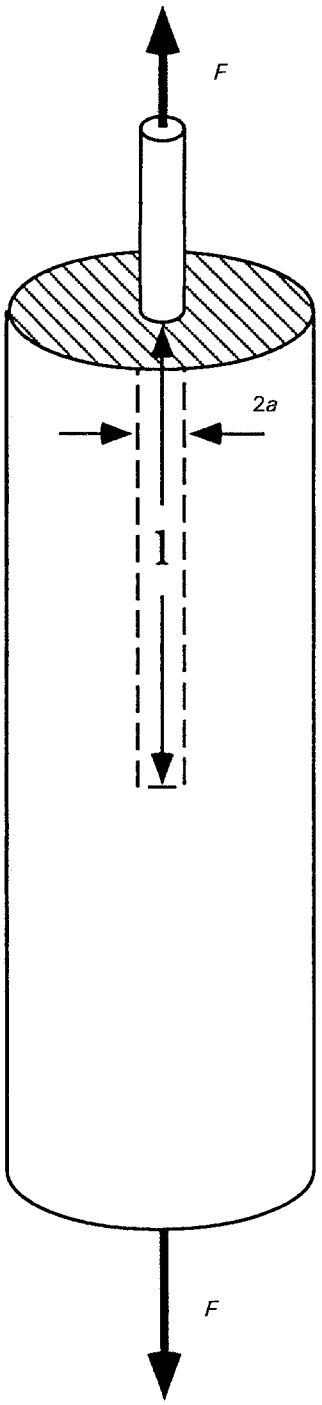

Figure 1 Pull-out of a long rod or fibre.

as a cylindrical debond propagates up the rod from the base. In other words, a partly-debonded rod having a length $(l - c)$ still bonded is assumed to have the same compliance as a bonded rod embedded to a depth $(l - c)$.

(d) The pull-out force, F_p, taken as the maximum force attained after cavitation had occurred; these forces are compared with those obtained from a simple fracture mechanics treatment outlined in Section 3.4, similar to one used previously to calculate fracture forces in related studies [1–6].

In the theoretical treatment, estimates are made of the elastic compliance, C, of the system as a function of length of debond, both by numerical calculation and by experiment. Then the rate of increase of compliance

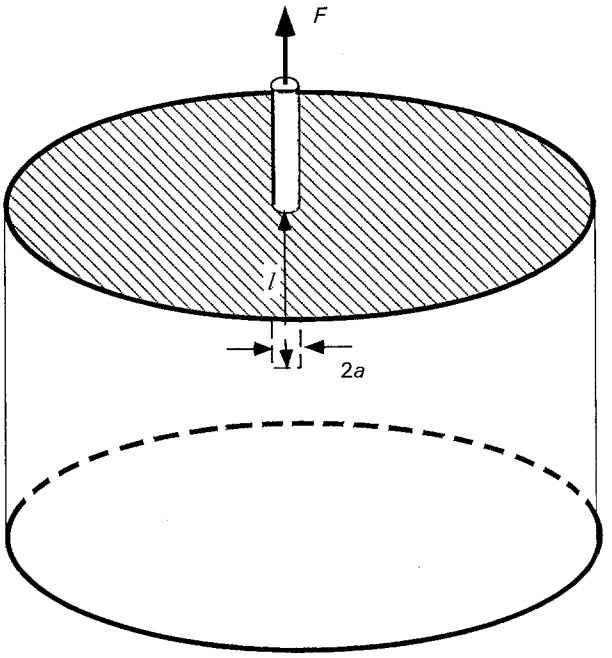

Figure 2 Pull-out of a short rod or fibre.

with debond area, A, is computed and used to calculate the critical condition for further debonding [7]

$$F^2 \geqslant 2G_a/(dC/dA) \quad (2)$$

Cavitation of rubber, on the other hand, appears to be described to a good approximation by a stress criterion [8–10]. When the local dilatant stress or negative hydrostatic pressure reaches a value similar in magnitude to the tensile modulus, E, then a large enclosed cavity appears suddenly, probably as a result of catastrophic growth by tearing of a precursor cavity, too small to see.

Finally, possible use of fibre pull-out as a test method for adhesion is discussed.

2. Experimental procedure

2.1. Preparation of samples

Rubber blocks, 100 mm long, 75 mm wide and 25 mm thick, were prepared by a moulding process using the following mix formulation in parts by weight: poly (ethylene-co-propylene) (Exxon EPM 404), 100; sulphur, 0.32; dicumyl peroxide, 2.7. Cross-linking was effected by heating the mix for 30 min at 140 °C followed by 60 min at 149 °C. The cross-linked rubber prepared in this way was sufficiently transparent for details of internal fractures to be observed through thicknesses of over 30 mm. The tensile (Young's) modulus was found to be 1.3 MPa using an indentation technique, as described in Section 3.1.

The upper plate of the steel mould used in preparing the rubber block held six cylindrical rods of extruded nylon, 3.18 or 6.35 mm in diameter, projecting into the mould by distances varying between 1.4 and 10 mm. They were located about 25 mm apart and at least 25 mm from an edge of the block in order to minimize edge effects or effects due to proximity to another rod. Before inserting them into the mould, the cylindrical sides and bottom surfaces of the rods were abraded

uniformly with 320 grit emery cloth. The sides were abraded in the axial direction only, to avoid making circumferential scratches or grooves. After roughening the surfaces in this way, the rods were rinsed, first with toluene and then with acetone, and allowed to dry before being inserted into the mould.

After being moulded under pressure in contact with the cleaned nylon rods, the rubber was found to adhere to them fairly strongly. Forces ranging from 10–50 N were required to pull the rods out completely. The work described here is a study of the mechanics of pull-out, focusing on the effects of embedded length and rod diameter. The level of adhesion per unit area is assumed to be constant. Frictional forces are neglected, because when a rod was re-inserted into the hole that it had been removed from, the pull-out force, now attributed solely to friction, was much smaller, only 3%–5% of the original value.

2.2. Measurement of adhesion

In order to measure the forces required to pull an embedded rod out of the block, it was necessary to secure the base of the rubber block firmly. This was accomplished by adhering the lower surface of the block to a thick aluminium baseplate treated with a two-coat adhesive system, consisting of a thin layer of Chemlok 205 (Lord Corporation), followed by a layer of Chemlok 236 (Lord Corporation). The lower surface of the cross-linked rubber block was cleaned by wiping it with toluene and then acetone. It was then pressed into contact with the coated baseplate for about 30 min at 105 °C. This procedure gave a bond sufficiently strong that it resisted rod pull-out forces, although the block could be removed using higher forces.

An alternative bonding system was also found to be satisfactory. After a layer of Chemlok 205 had been applied to the baseplate, a layer of Epituf 37–40 epoxy resin (Reichhold Chemical Company) containing tetraethylene pentamine curing agent was applied. Bonding to the rubber block was effected at a temperature of about 100 °C.

The baseplate was fastened to the crosshead of a tensile testing machine and the nylon rods were pulled out of the rubber block successively, at a speed of about 4 $\mu m\,s^{-1}$. Force measurements were recorded continuously during pull-out.

2.3. Observation of internal failures

A high-intensity microscope lamp was placed behind the block and a cathetometer was positioned in front, to measure the displacement of the rod as a function of applied force and to study the progress of internal fractures. To minimize surface scattering, the front side of the block was coated with a thin layer of silicone oil.

3. Results and discussion

3.1. Tensile modulus of the rubber

Relations were obtained between applied force, F, and indentation, d, using extra specimens of the flat-ended nylon rods as indentors. The relations were quite linear over the range of indentation used, up to about 1 mm. For materials that are incompressible in bulk, the theoretical relation between force and indentation is [11]

$$F = 8Ead/3 \quad (3)$$

where a is the indentor radius. Values of Young's modulus, E, were calculated from the forces at 0.75 mm indentation and found to be 1.25 ± 0.03 MPa using rods of 3.18 mm radius and 1.35 ± 0.03 MPa using rods of 1.59 mm radius. A mean value of 1.3 MPa was therefore adopted. This is consistent with measurements on fully bonded rods, described in Section 3.4.

3.2. General features of pull-out

A typical experimental relation between pull-out force, F, and displacement, d, of the rod is shown schematically in Fig. 3. There are essentially two regions, corresponding to two different processes. At first, the force–displacement relation was substantially linear until a critical condition was reached, at a maximum force, denoted F_c. At this point a cavity appeared in the rubber below the end of the rod, close to, but apparently separate from the rod. It was generally located at the edge of the flat end surface, as shown schematically in Fig. 4a. After appearing, the cavity spread rapidly across the flat surface of the rod, Fig. 4b, until the entire end surface appeared to be debonded, Fig. 4c. Meanwhile the force dropped to a minimum value, denoted F_s.

On continuing to pull the rod, the force increased linearly with displacement, as shown schematically in Fig. 3, but now with a lower slope than before, until at a critical force, denoted F_p, the rod became fully detached. At most, a small frictional force was necessary to complete the separation.

These two processes, cavitation and debonding of the rod end, and pull-out of a rod with the embedded end already debonded, are now discussed separately.

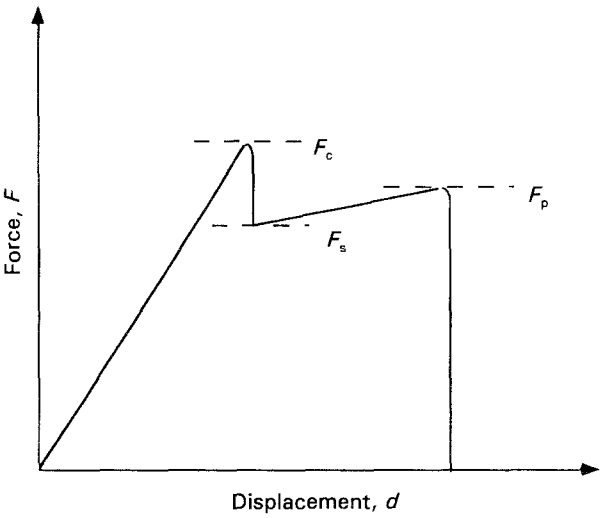

Figure 3 Schematic relation between pull-out force, F, and rod displacement, d.

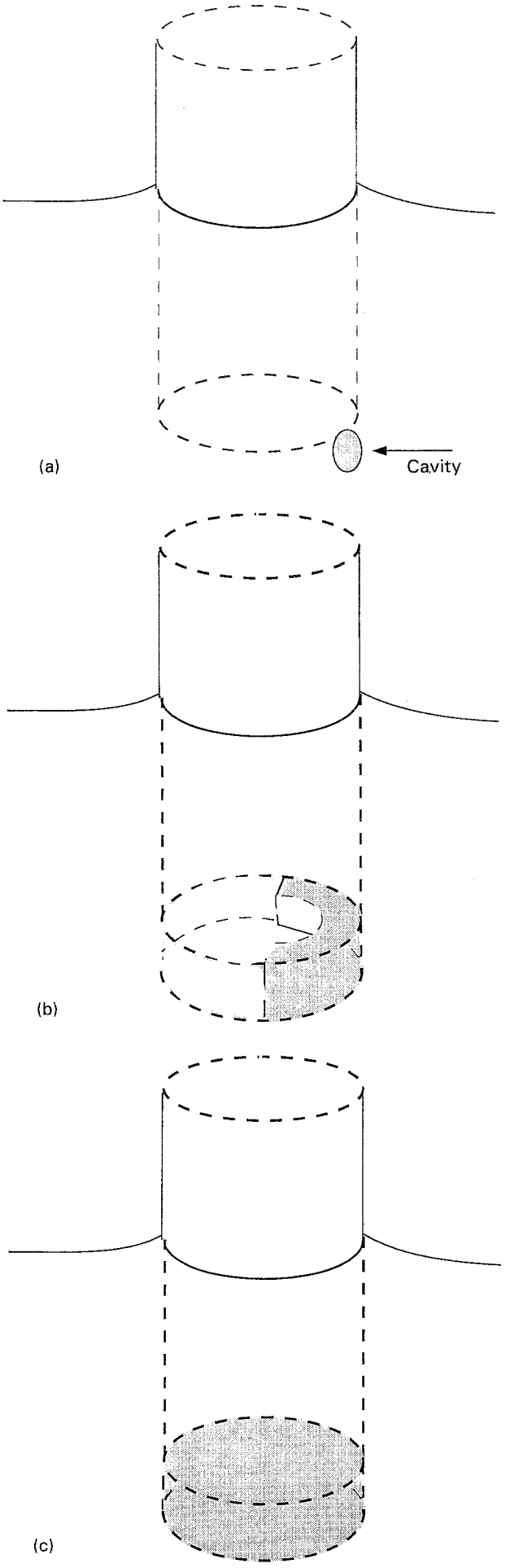

Figure 4 Sketch of cavitation and detachment under the rod base. (a) Start of cavitation, (b) spreading of a debond, (c) complete separation.

3.3. Cavitation and debonding at the embedded end

The present observations of the appearance and growth of cavities near the rod end are strikingly similar to those made previously using wholly embedded rods [12]. It is assumed that the critical parameter is the local dilatant stress or negative hydrostatic pressure. Finite element calculations revealed that the highest dilatant stress was set up near the edge of the rod and cavities first appeared in this region [12]. The same phenomenon appears to occur with partly embedded rods. We assume that the same fracture criterion is operative, i.e. that the dilatant stress first reaches a value close to the tensile (Young's) modulus, E, of the rubber in this region.

In the present case, the force for cavity initiation was found to increase linearly with embedded length of rod, Fig. 5. Thus, the experimental relations can be described by

$$F = 25 + 4300l \quad (4)$$

where F is in Newtons and l in metres, or

$$\bar{\sigma}/E = F/(E\pi a^2) = 0.6 + 0.35(l/a) \quad (5)$$

for rods of 3.18 mm radius, and

$$F = 8 + 3200l \quad (6)$$

again with F in Newtons and l in metres, or

$$\bar{\sigma}/E = F/(E\pi a^2) = 0.8 + 0.5(l/a) \quad (7)$$

for rods of 1.59 mm radius, where $\bar{\sigma}$ denotes the mean applied tensile stress. Extrapolated values at zero embedded length correspond to values expected for cavity formation beneath flat-ended rigid discs adhering to the surface of an elastic half-space of an incompressible material and pulled upwards. The

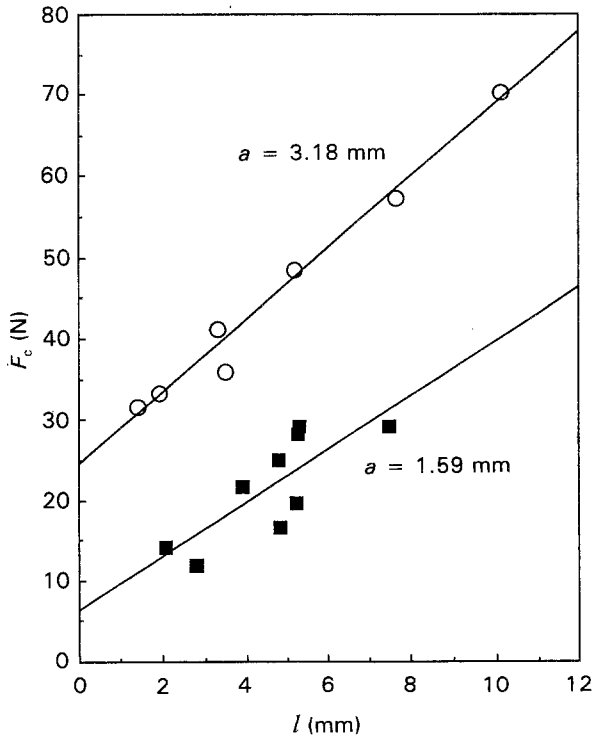

Figure 5 Cavitation force, F_c, versus depth, l, of embedment.

mean tensile stress, $\bar{\sigma}$, set up beneath a rigid disc is $F/\pi a^2$, and the triaxial tension in the centre of the contact circle is one-half of this amount [11]. However, the tensile stress rises towards the edge of the contact circle, reaching a theoretically infinite value at the edge. It seems likely that the triaxial tension rises similarly towards the edge, as found before [12]. An effective value in the edge region is assumed to be about twice the minimum, i.e. equal to the mean tensile stress. For the two rods examined, the critical applied stresses were then approximately equal, 0.6–0.8 MPa, i.e. about two-thirds of the tensile modulus of the rubber. In view of uncertainties in the actual hydrostatic tension set up, these values are close enough to the general criterion for cavity formation in rubbery solids to suggest that the same criterion holds under an embedded rod or adhering disc.

3.4. Stiffness of blocks with embedded rods

The rise in critical force with depth of embedment, Fig. 5, indicates that part of the applied force is taken up by shear stresses acting at the cylindrical surface of the rod. Only a fraction acts on the adhering material at the base and creates the hydrostatic tension there necessary to cause cavitation. Thus, a continuous increase in stiffness is expected with increasing depth of embedment.

Measurements were made of the stiffness, S, for a fully bonded rod as a function of the depth, l, of embedment, where S is given by the slope of the force–displacement relation before any cavitation. As shown in Fig. 6, the measured values of S increased linearly with l, following relations of the form

$$S/Ea = A_1 + B_1(l/a) \quad (8)$$

where the coefficients A_1 and B_1 are 3.4 and 1.15, respectively, for rods of 3.18 mm radius, and 2.9 and 1.1, respectively, for rods of 1.59 mm radius. These values can be compared with those obtained from an approximate finite element calculation described in the Appendix: $A_1 = 3.15$, $B_1 = 1.9$ for 3.18 mm rods; and $A_1 = 2.85$, $B_1 = 1.1$ for 1.59 mm rods. The finite element analysis (FEA) results are quite similar to the experimental values and confirm that the stiffness does indeed increase linearly with depth of embedment, and that the coefficients B_1 describing this dependence are not equal for rods of different radius. (The reason for this feature is discussed later.)

Values of reduced stiffness S/Ea at zero embedded depth, given by the coefficients A_1, can be compared with the theoretical value of 2.67 for a flat-ended indentor, Equation 3. They are in reasonably good agreement.

Stiffness values, S', were also determined from the residual force, F_s, remaining after cavitation was complete and the rod end was fully debonded. As shown in Fig. 7, S' also increased linearly with depth of embedment, for rods of both radii

$$S'/Ea = A_2 + B_2(l/a) \quad (9)$$

where the coefficients A_2 and B_2 are 1.65 and 1.1, respectively, for rods of 3.18 mm radius, and 1.65 and 0.9, respectively, for rods of 1.59 mm radius. These values are again in reasonably good agreement with those obtained by FEA: $A_2 = 1.95$, $B_2 = 1.8$ for

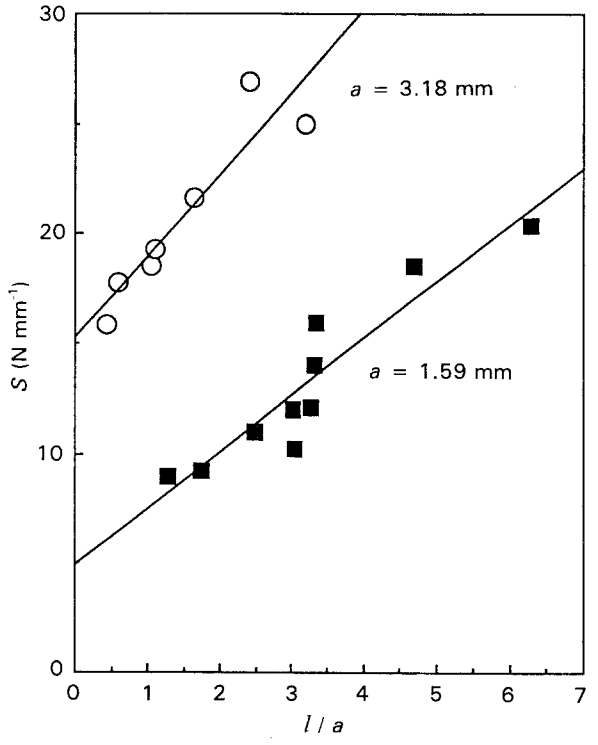

Figure 6 Stiffness, S, versus depth, l, of embedment for fully bonded rods.

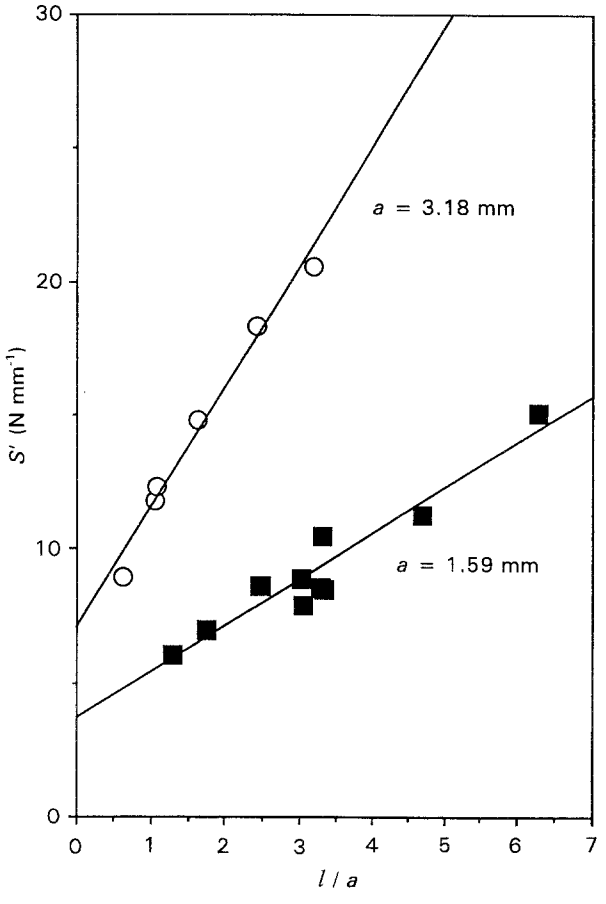

Figure 7 Stiffness, S', versus depth, l, of embedment for rods with the embedded ends unbonded (due to cavitation).

3.18 mm rods; and $A_2 = 1.95$, $B_2 = 1.1$ for 1.59 mm rods, see Appendix. Again, both sets of results indicate that the stiffness after cavitation increases linearly with depth, l, of embedment, and that the coefficients B_2 are not constant but depend upon the rod radius.

At this point it is sufficient to note that the relevant values of the elastic constants A_2 and B_2 are readily determined for any combination of rod and block dimensions, either by experiment or by numerical calculation, for use in the theoretical treatment outlined in the following section.

3.5. Pull-out forces

Empirically, the stiffness S' after the flat end of a rod is debonded is given by a relation of the form of Equation 9. We assume that the stiffness after a cylindrical debond of length c has grown up the rod, starting from the embedded end, is given by the same relation with l replaced by $(l - c)$. Thus, the rate of increase of compliance C ($= 1/S'$) with area A ($= 2\pi ac$) of debond is $EB_2/2\pi a(S')^2$. On substituting in Equation 2, the pull-out force, F_p, is obtained as

$$F_p^2 = 4\pi aEG_a[A_2a + B_2(l - c)]^2/B_2 \quad (10)$$

Equation 10 predicts a linear dependence of pull-out force F_p upon the depth, l, of embedment. In agreement with this, experimental values were found to be in reasonable accord with linear relations, Fig. 8.

The extrapolated value of F_p for rods of infinitesimally short embedment depth is predicted to be

$$F_p^2(l \to 0) = 4\pi a^3EG_aA_2^2/B_2 \quad (11)$$

These two results, Equations 10 and 11, provide, in principle, two independent ways of deducing the strength, G_a, of the interface from measurements of pull-out force, F_p. Using the slopes and intercepts of the linear relations shown in Fig. 8, values of G_a were calculated from Equations 10 and 11. They are given in Table I. The values are all similar in magnitude, both from the slopes and intercepts of measurements with each rod radius, and also for rods of different radii, being about 210 $J\,m^{-2}$ in one case and about 320 $J\,m^{-2}$ in the other. These are quite reasonable values for weak bonds and suggest that the pull-out analysis proposed is basically correct.

TABLE I Values of fracture, energy, G_a, derived from measured pull-out forces, F_p, using Equations 10 and 11

	a (mm)	
	3.18	1.59
$F_p\,(l - 0)$ (N)	14.5	6.8
dF_p/dl ($N\,mm^{-1}$)	3.9	3.2
G_a ($J\,m^{-2}$) (Eq. 10)	205	265
G_a ($J\,m^{-2}$) (Eq. 11)	210	375

The lower values obtained with large-radius rods might be due to the higher forces needed to induce cavitation then. Pull-out followed soon after and, in some cases, partial debonding of the cylindrical surface of the rod may have occurred simultaneously, so that the actual pull-out force was hidden by the higher force needed for cavitation. If pull-out experiments were to be used as a method of determining G_a it would be advisable to use small-radius rods in order to avoid this complexity. Alternatively, cavitation could be prevented altogether by treating the rod base with a release agent to prevent bonding over the flat end. Only the pull-out force would be observed then.

It would also be necessary to adopt standard dimensions for the elastic block in view of the unexpected effect that the block size has on the elastic coefficient B_2 in particular, and hence on the expected pull-out force. Indeed, it is interesting to speculate what results would be obtained if the block dimensions were to be made extremely large in comparison with the length and radius of an embedded rod. From FEA calculations it seems likely that contributions to stiffness from embedment would approach zero in this case. Thus, only the force required to detach the rod end would be necessary for pull-out.

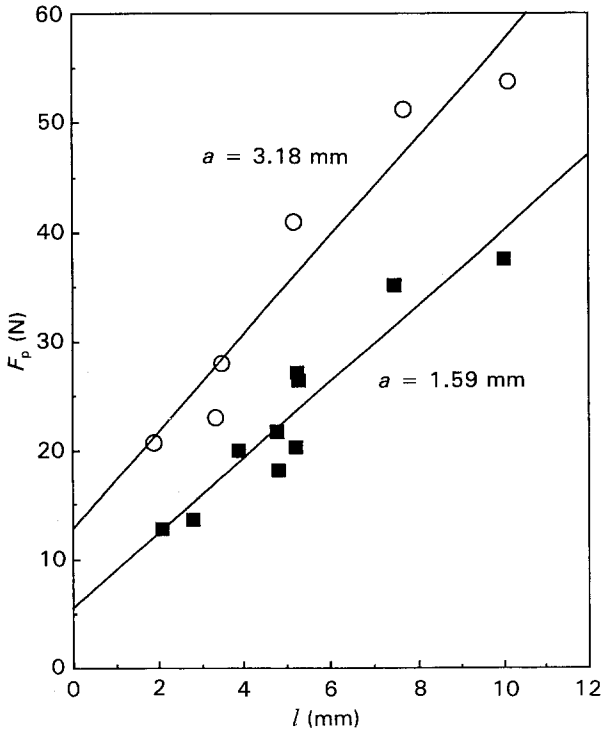

Figure 8 Pull-out force F_p versus depth, l, of embedment.

4. Conclusions

Pull-out stiffness for a rigid rod embedded in an elastic block increases linearly with depth of embedment, both for a fully bonded rod and for one with its flat base unbonded. This result is obtained both experimentally and by FEA.

Surprisingly, the dependence on depth of embedment varies with the dimensions of the block in which the rod is embedded, even when the block is many times larger than the rod. Empirical relations for this effect have been obtained by FEA. Although limited to only two sizes of rod, experimental results are in reasonably good quantitative accord with the theoretical predictions.

As a rod is being pulled out, a cavity appears suddenly within the rubber under the flat lower surface of the rod, generally near the edge, at a critical value of applied force. This cavity grows and spreads over the lower surface of the rod and effectively debonds it from the rubber. Forces for cavity initiation are in reasonable accord with a critical value of hydrostatic tension within the rubber, approximately equal to the tensile modulus, E.

Forces for subsequent pull-out are in reasonable agreement with a simple fracture mechanics treatment based on the empirically determined linear relations referred to above for pull-out stiffness as a function of embedment depth. The value deduced for the fracture energy of the interface in this way is 200–300 $J\,m^{-2}$ from two independent measures, using two rod radii. This general agreement suggests that the basic mechanics of pull-out of relatively short rods has been taken into account.

Acknowledgements

This work was started during a programme of research on the mechanics of composites supported by the Office of Naval Research (Grant N00014-85-K-0222, Contract Officer Dr R. S. Miller). The experiments were carried out at The University of Akron as part of an MS degree research project in polymer science and are described in full elsewhere (C. L. Shambarger, MS thesis, The University of Akron, 1975). The authors thank Mr R. H. Finney and Mr A. Kumar of HLA Engineers, Inc., Dallas, Texas, for kindly supplying the TEXPAC-L FEA Program and advising on its use.

References

1. A. N. GENT, G. S. FIELDING-RUSSELL, D. I. LIVINGSTON and D. W. NICHOLSON, *J. Mater. Sci.* **16** (1981) 949.
2. A. N. GENT and O. H. YEOH, *J. Mater. Sci.* **17** (1982) 1713.
3. A. N. GENT and S. Y. KAANG, *Rubb. Chem. Technol.* **62** (1989) 757.
4. A. N. GENT and G. L. LIU, *J. Mater. Sci.* **26** (1991) 2467.
5. A. N. GENT and C. WANG, *ibid.*, **28** (1993) 2494.
6. *Idem, ibid.* **27** (1992) 2539.
7. J. G. WILLIAMS, "Fracture Mechanics of Polymers" (Wiley, New York, 1984) p. 30.
8. A. N. GENT and P. B. LINDLEY, *Proc. Roy. Soc. (Lond.)* **A249** (1958) 195.
9. A. E. OBERTH and R. S. BRUENNER, *Trans. Soc. Rheol.* **9** (2) (1965) 165.
10. A. N. GENT and D. A. TOMPKINS, *J. Appl. Phys.* **40** (1969) 2520.
11. S. P. TIMOSHENKO and J. N. GOODIER, "Theory of Elasticity", 3rd Edn (McGraw-Hill, New York, 1970) p. 408.
12. K. CHO, A. N. GENT and P. S. LAM, *J. Mater. Sci.* **22** (1987) 2899.
13. "TEXPAC-L", a small finite-element program designed for use on personal computers, provided by R. H. Finney, HLA Engineers, Inc., Dallas, Texas (1993).

Appendix: FEA calculations of stiffness

Calculations of stiffness S, S' for embedded rods, assuming linear elastic behaviour of the rubber block, were carried out using a small finite-element programme [13]. A cylindrically symmetrical grid was used, illustrated in Fig. A1. Eight-noded quadrilateral elements were employed, scaled progressively in width from the centre outwards by a final factor of up to tenfold. Dimensions of the rubber block were chosen to be 150 mm radius and 200 mm depth, the outer cylindrical surface and bottom flat surface being prevented from any displacement radially or axially. The rod radius, a, and depth, l, of embedment were varied over wide ranges. The tensile modulus of the rubber cylinder was given a value of 1.1 MPa and the bulk modulus a value of 15 000 MPa, making the rubber virtually incompressible. The rods were assigned a tensile modulus of 200 000 MPa, making them effectively rigid. For rods having fully formed cavities underneath them, the tensile and bulk moduli of elements immediately under the base of the rod were given values close to zero.

In all cases, the stiffnesses S and S' were found to be linearly dependent upon the depth, l, of embedment of the rod. A representative plot is shown in Fig. A2. Values of the coefficients A_1, B_1, A_2, B_2 in Equations 8 and 9 were obtained from the intercepts and slopes of such relations. They are listed in Table II and plotted in Figs A3 and A4 as functions of the ratio, a/R, of rod radius to the external radius, R, of the rubber cylinder in which it was embedded. The following features are noteworthy.

First, values of the coefficient A_1 appear to approach the theoretical value of 8/3 for rods of sufficiently small radius, but it is surprising how small the radius must be to give accurate results – when the rod

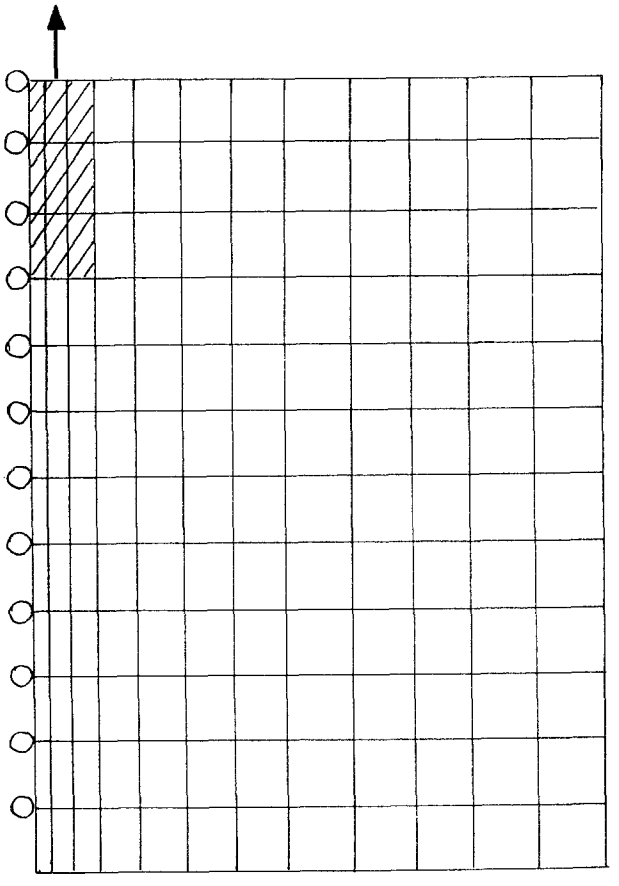

Figure A1 Grid used for finite-element calculations.

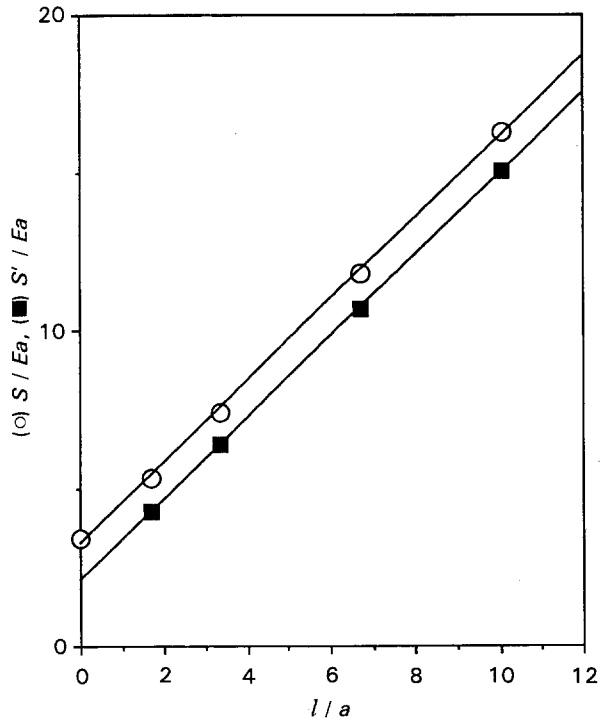

Figure A2 Representative plots of reduced stiffness S/Ea from FEA calculations versus depth, l, of embedment. $a/R = 0.08$.

TABLE AI Values of coefficients A_1, A_2, B_1, B_2 in Equations 8 and 9, determined by FEA

a/R	A_1	A_2	B_1	B_2
0.080	3.0	2.1	1.33	1.29
0.118	2.9	1.8	1.87	1.705
0.172	3.5	1.95	2.55	2.20
0.234	4.1	1.85	3.6	2.95
0.333	5.2	2.1	7.1	4.2

radius was 10% of the cylinder radius, then the error in A_1 was about 10%. This error is attributed to edge effects. Secondly, the coefficient A_2 was rather independent of the ratio a/R up to a value of 0.33, with an average value of 1.95. Apparently, edge effects are less important when the rod base is unbonded. Values of the coefficients B_1 and B_2 were approximately equal for small-radius rods, and appeared to extrapolate to a value of about 0.7 as the ratio a/R approached zero. However, both coefficients depended strongly upon the ratio a/R over the entire range examined, Fig. A4, especially B_1.

This strong effect of the external radius, R, of the rubber cylinder (and presumably of the block depth, L, as well) upon the stiffness of embedded rods indicates that it will be difficult in practice to choose sample dimensions such that the stiffness is independent of the size of the block in which it is embedded.

In the present experiments the spacing between rods was about the same as the block depth, L, i.e. 8 or 16 times the rod radius, a. Assuming that proximity to other rods or to the bonded base has a similar effect as proximity to an external wall, relevant values of the elastic coefficients can be read from Figs A3 and A4. The appropriate ratios a/R for the two rod radii used are 0.065 and 0.13, corresponding to values for A_1 of

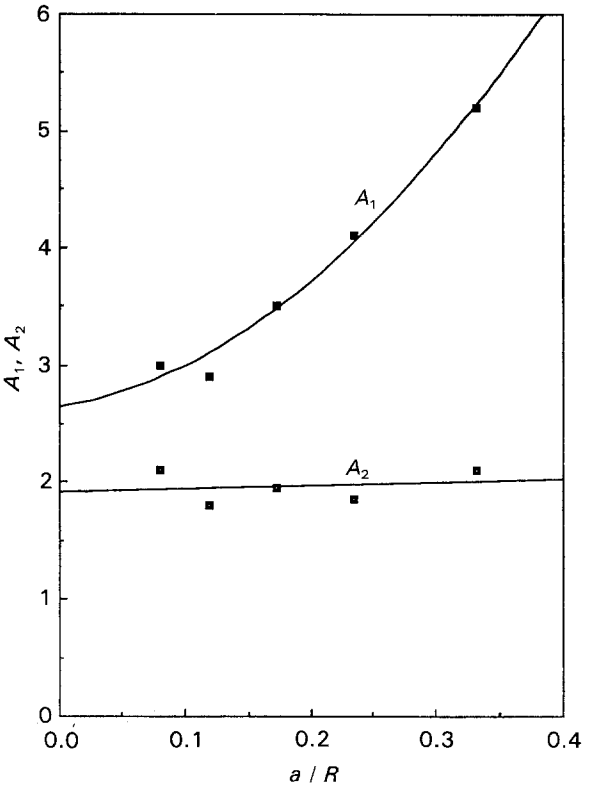

Figure A3 Coefficients A_1, A_2 in Equations 8 and 9 from FEA results versus ratio of rod radius a to external radius R of rubber block.

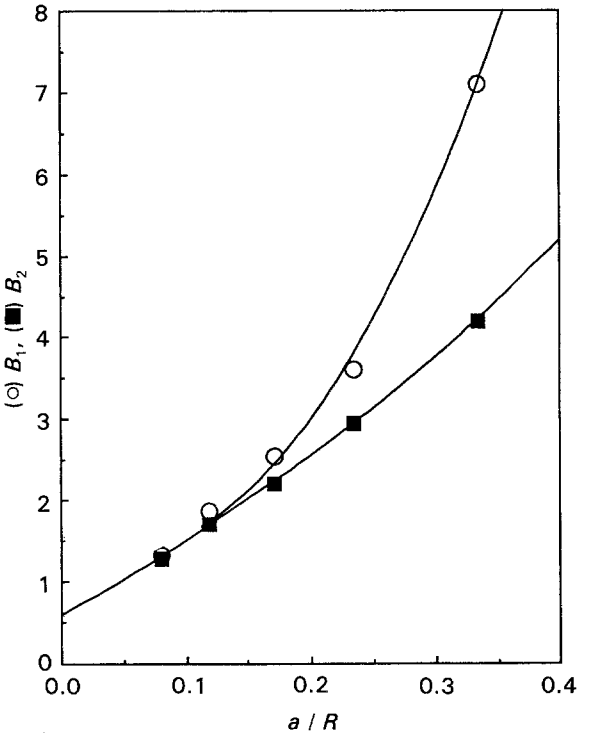

Figure A4 Coefficients B_1, B_2 in Equations 8 and 9 from FEA results versus ratio of rod radius, a, to external radius, R, of rubber block.

2.85 and 3.15, for A_2 of 1.95 and 1.95, for B_1 of 1.1 and 1.9, and for B_2 of 1.1 and 1.8, respectively. These values are quite similar to those observed experimentally, Figs 6 and 7.

Received 19 April
and accepted 16 August 1993